Original Research

Correction of Phase Offset Errors in Main Pulmonary Artery Flow Quantification

Jan-Willem Lankhaar, MSc,[1]* Mark B.M. Hofman, PhD,[1] J. Tim Marcus, PhD,[1]
Jaco J.M. Zwanenburg, MSc,[1] Theo J.C. Faes, MSc, PhD,[1]
and Anton Vonk-Noordegraaf, MD, PhD[2]

Purpose: To investigate whether an existing method for correction of phase offset errors in phase-contrast velocity quantification is applicable for assessment of main pulmonary artery flow with an MR scanner equipped with a high-power gradient system.

Materials and Methods: The correction method consists of fitting a surface through the time average of stationary pixels of velocity-encoded phase images, and subtracting this surface from the velocity images. Pixels are regarded as stationary if their time standard deviation falls into the lowest percentile. Flow was measured in the main pulmonary artery of 15 subjects. Each measurement was repeated on a stationary phantom. The phase offset error in the phantom was used as a reference. Correction was applied with varying polynomial surface orders (0–5) and stationarity percentiles (5–50%). The optimal surface order and stationarity percentile were determined by comparing the fitted surface with the phantom.

Results: Using a first-order surface and a (noncritical) 25% percentile, the correction method significantly reduced the phase offset error from 1.1 to 0.35 cm/second (RMS), which is equivalent to a reduction from 11% to 3.3% of mean volume flow. Phase error correction strongly affected stroke volume (range –11 to 26%).

Conclusion: The method significantly reduces phase offset errors in pulmonary artery flow.

Key Words: phase-contrast velocity quantification; phase offset error; phase error correction; eddy-current–induced fields; stroke volume; pulmonary blood flow
J. Magn. Reson. Imaging 2005;22:73–79.
© 2005 Wiley-Liss, Inc.

IN MR CINE phase-contrast velocity quantification, the velocity-encoded phase images can be distorted by non-

compensated eddy-current–induced fields and concomitant gradient terms (1,2). These result in phase offset errors that can be recognized by nonzero velocity of stationary tissue (2). As volume flow assessment in the large vessels is determined by integration over time and space, relatively small velocity offsets can lead to significant errors in mean volume flow, stroke volume, and cardiac output. Most scanners are designed to compensate for the induced fields, but with the recent advent of high-power gradient systems the problem of phase offset errors has again become more prominent (1).

For correction of phase offset errors, several postprocessing methods exist (2). Most commonly, the offset is estimated from a region of stationary tissue (3,4), but due to spatial variation of the offset this region has to be near the vessel of interest. This method does not work for flow quantification in the great vessels near the heart because of the lack of stationary tissue in the vicinity of the heart. One solution is to perform a separate acquisition on a stationary phantom to determine the phase offset at the location of the vessel (3). However, this acquisition has to be repeated for each individual case, as the slice orientation influences the phase offset. Therefore, this solution is inconvenient in clinical practice. Another solution is to assume that the phase error exhibits a smooth spatial variation and to estimate the spatial distribution of the complete velocity image (5). A specific implementation of this method, proposed by Walker et al (6), has been frequently applied (7,8). Assuming that phase offset errors exhibit linear spatial dependency, they estimated the phase offset errors by fitting a flat surface through the velocities in all stationary tissue of the image, and subtracting the surface from the velocity image. The method was proposed in 1993 and was originally used for reduction of phase offset errors in in-plane velocity quantification. Since then, the power of gradient coils of MR scanners has increased, resulting in larger phase offset errors.

The method of Walker et al (6) seemed to work well when it was originally proposed. It is clear, however, that it was not designed for correction of phase offset errors due to concomitant gradient terms, as the importance of these terms for velocity quantification was not quantified until the late 1990s (1). In the presence of concomitant gradient phase offset errors, a linear sur-

face would not suffice because the lowest order of these errors is quadratic, but because their physical origin is well understood they can be corrected analytically in the reconstruction (1). Doubt has existed as to whether the method is useful for correction of phase offset errors that remain after correction for concomitant gradient terms. In an in vitro study, Greil et al (7) applied the method to velocity images of a pulsatile flow phantom that had been corrected for concomitant gradient terms. They found no significant reduction of the errors, but they did not test whether correction in vivo would yield the same results.

In this study, a variant of the method of Walker et al (6) was evaluated for clinical measurement of stroke volume and mean volume flow in the main pulmonary artery of patients with various forms of pulmonary hypertension and healthy volunteers. An MR scanner with a high-power gradient system was used, and the correction method was applied after compensation for phase errors due to concomitant gradient terms. In particular, we studied whether a linear or a higher-order surface should be used, and which threshold is optimal for discriminating stationary from nonstationary tissue. The velocities measured in a stationary phantom with the same acquisition parameters as in the patient were a measure for the true phase offset errors in the patient (3,9,10).

MATERIALS AND METHODS

Phase Offset Error Correction

Phase Offset Error in Stationary Tissue

In through-plane phase-contrast flow quantification, the pixel value of the phase images is proportional to the velocity component perpendicular to the imaging plane. If blood or tissue at position (x,y) in frame t_i has a true velocity component perpendicular to the imaging plane $v(x,y,t_i)$, and a phase offset error $v_{off}(x,y,t_i)$, the actually measured velocity $\hat{v}(x,y,t_i)$ equals

$$\hat{v}(x,y,t_i) = v(x,y,t_i) + v_{off}(x,y,t_i) + \varepsilon(x,y,t_i) \quad (1)$$

with $\varepsilon(x,y,t_i)$ zero-mean noise. In stationary tissue, $v(x,y,t_i)$ equals zero. Hence, $\hat{v}(x,y,t_i)$ and $v_{off}(x,y,t_i)$ are approximately equal. If, furthermore, the phase offset error is constant during the cine, the signal-to-noise ratio can be improved by temporally averaging the velocity in stationary tissue.

Therefore, assuming that the phase offset error is constant during the cine, an estimate of the error in stationary tissue can be obtained from the temporally averaged velocity of stationary tissue $\bar{v}_{stat}$

$$\bar{v}_{stat}(x,y) = \frac{1}{N}\sum_{i=1}^{N}\hat{v}_{stat}(x,y,t_i)$$

$$= v_{off}(x,y), \text{ all } (x,y) \text{ in stationary tissue} \quad (2)$$

with N the number of frames in the cine. In the original method the latter averaging was not applied, but the

phase offset error in stationary tissue was estimated for each time frame separately (6).

Phase Offset Error in Nonstationary Tissue

Phase offset errors of different sources are known to exhibit a smooth spatial dependence (1,5,11). This property allows estimation of the phase offset error in nonstationary pixels from a surface fit through the phase offset error in stationary pixels. By subtracting the fitted surface from the phase image, the phase offset errors are corrected.

The unknown, not necessarily flat, surface $S(x,y)$ can be approximated by a two-dimensional Taylor expansion of order k

$$S(x,y) = \sum_{i=0}^{k}\sum_{j=0}^{i}a_{ij}x^{i-j}y^j =$$

$$a_{00} +$$
$$a_{10}x + a_{11}y +$$
$$a_{20}x^2 + a_{21}xy + a_{22}y^2 +$$
$$\vdots$$
$$a_{k0}x^k + a_{k1}x^{k-1}y + \ldots + a_{kk}y^k \quad (3)$$

with a_{ij} unknown parameters. Because Eq. [3] is linear in the parameters a_{ij}, an ordinary least-squares method can be used to estimate them for a specified order k. Originally, order $k = 1$ was used and the least-squares problem for this linear surface was solved analytically (6). We estimated S for different values of k and used MATLAB's standard least-squares algorithm (12). In order to improve numerical accuracy, the pixel values of the phase image and the x and y coordinates were converted to double precision.

In case of spatial aliasing (infolding) artifacts, the spatial dependence is distorted. This generally leads to a surface fit of higher order than intrinsically necessary for the real phase offset error. Areas with spatial aliasing artifacts were therefore manually excluded from the surface fit.

Selection of Stationary Tissue

For the surface fit, it is necessary to discriminate stationary from nonstationary pixels. By definition, stationary pixels exhibit little or no variation in $v(x,y,t_i)$ during the cine. Therefore, the (time) standard deviation, a measure of variation, was used to select the stationary pixels. The standard deviation $\sigma(x,y)$ at pixel (x,y) equals

$$\sigma(x,y) = \sqrt{\frac{1}{N-1}\sum_{i=1}^{N}(\hat{v}(x,y,t_i) - \bar{v}(x,y))^2} \quad (4)$$

with $\bar{v}(x,y)$ the time average of $\hat{v}(x,y,t_i)$.

Pixels were regarded stationary if $\sigma(x,y)$ was below a certain threshold value. This threshold value was chosen such that the lowest percentile of the standard deviations, λ, was regarded as stationary. If, for example, the user chose to include 50% of all pixels ($\lambda = 0.5$),

the threshold was the median value of $\sigma(x,y)$. Originally, a stationarity percentile of 15% was suggested (6).

Order and Percentile Selection

The performance of the correction method, for a particular surface order k and percentile λ, was assessed as follows. The estimated offset $S_{k,\lambda}(x,y)$ was spatially averaged across the pulmonary artery cross-section, and was compared with the velocity of a stationary phantom acquisition spatially averaged across the same region. This phantom measurement, acquired with the same acquisition parameters and image orientation as the subject's measurement, was regarded as the reference. Thus, the performance $\delta_{k,\lambda}$ was defined as

$$\delta_{k,\lambda} = |\bar{S}_{k,\lambda} - \bar{v}_{\text{phant}}| \qquad (5)$$

with $\bar{S}_{k,\lambda}$ the estimated offset and $\bar{v}_{\text{phant}}$ the velocity in the phantom, both averaged across the vessel cross-section.

The surface order was varied from $k = 0$ to 5 (with $k = 0$ the mean value of the stationary pixels). For each order, λ was varied from 0.05 to 0.50 of the pixels, with steps of 0.05. For each k and λ, the performance $\delta_{k,\lambda}$ was calculated.

Acquisitions

In a group of 13 patients (mean age 51 years, eight male) with various forms of pulmonary hypertension, and two healthy subjects (one male, age 29 years; one female, age 65 years) flow was measured in the main pulmonary artery using phase-contrast velocity quantification. A 1.5-T whole body scanner (Magnetom Sonata; Siemens Medical Systems, Erlangen, Germany) equipped with a 40 mT/m gradient coil and a 200 T/m.second slew rate was used. For the volunteer acquisitions, informed consent was obtained according to the rules of the ethical committee of our center.

MR phase-contrast velocity measurements were performed as follows. On a sagittal scout image, an oblique plane perpendicular to the main pulmonary artery was positioned. A two-dimensional spoiled gradient-echo pulse sequence was applied with an excitation angle of 15°, a TE of 4.8 msec, TR of 11 msec, and a receiver bandwidth of 170 Hz per pixel. One-dimensional velocity-encoding was performed perpendicular to the imaging plane. Velocity sensitivity was set to 120 cm/second, but, if appropriate, this was adjusted to lower or higher values in individual cases. The velocity encoding was interleaved, resulting in a temporal resolution of 22 msec. The field of view was set to 260×320 mm, and the matrix size to 208×256. No k-space segmentation was applied and acquisitions were not averaged. In the reconstruction, the Maxwell concomitant gradient terms were corrected to the order $1/B_0$ (1). The acquisition was prospectively triggered to the electrocardiogram (ECG), and during the acquisition, the patients breathed freely. This flow measurement is part of the MR protocol that is included in the clinical work-up of patients with pulmonary hypertension in our center (13).

Directly after the patient acquisition, the acquisition was repeated (with identical acquisition parameters and image orientation, but without ECG triggering) on a stationary fluid-filled phantom. In order to increase the signal-to-noise ratio, five or 10 acquisitions were averaged.

Data Analysis

Flow analysis in the main pulmonary artery was performed with Medis Flow (version 3.1β; Medis, Leiden, the Netherlands). Contours surrounding the vessel cross-section were drawn in the magnitude image. Spatial wrapping artifacts were manually excluded from the surface fit, by enclosing them in another contour.

For determination of the optimal combination of surface order and stationarity percentile (k,λ), the performance $\delta_{k,\lambda}$ was investigated using a univariate analysis of variance (ANOVA) with Bonferroni correction. Subject was treated as a random factor in order to control interindividual variation, while k and λ were treated as fixed factors. A two-way interaction of k and λ was also included in the model. In order to stabilize variance, log $\delta_{k,\lambda}$ was used as a response variable.

A paired t-test was performed for comparison of the average error in the vessel cross-section before and after phase offset error correction with the optimal k and λ. To study the effect of phase offset error correction on mean volume flow and stroke volume, both quantities were derived from the subjects' volume flow curves before and after correction. Stroke volume was calculated from the systolic phase of the volume flow curve (forward flow only).

Both phase offset error correction and performance analysis were conducted with MATLAB (version 7.0.0, R14) (12). Statistical analysis was conducted with SPSS (version 10.0 for Windows).

Check of Assumptions

A simple check of the phantom measurement as a standard for offset determination was made by comparing the velocities in the phantom and in stationary tissue. The stationary tissue was identified in the patient acquisition (with $\lambda = 0.35$). Subsequently, all cardiac tissue and regions of ghosting were excluded manually to make sure that all the selected pixels represented stationary tissue. From this selection, the pixels located within the phantom cross-section were identified. The spatial and time average velocity of these pixels was compared with the spatial average velocity of the corresponding pixels in the phantom acquisition.

Stationarity of the phase offset errors, assumed for the time-independent variant of the correction method, was checked by plotting the spatial average of the selected stationary pixels ($\lambda = 0.25$) in each acquisition as a function of time.

RESULTS
Order and Percentile Selection

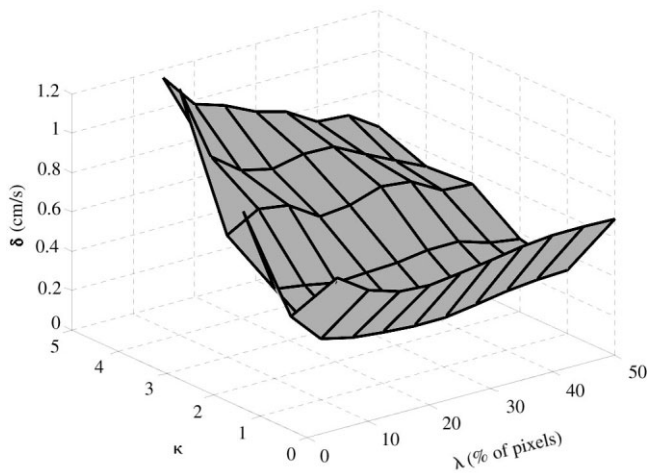For determination of the optimal combination of surface order k and stationarity percentile λ, the absolute

Figure 1. Absolute difference between estimated and reference offset (δ) as a function of surface order (k) and percentile (λ), averaged over all subjects. For $k = 1$ and $\lambda = 0.25$, δ is minimum. Differences greater than 1.5 cm/second (for high surface orders and low percentiles) have been omitted from the plot.

Figure 3. A pulmonary artery flow curve before and after phase error correction.

difference between the estimated and the reference velocity $\delta_{k,\lambda}$ was calculated for all combinations in all patients. In Fig. 1, $\delta_{k,\lambda}$ averaged over all subjects, is shown as a function of k and λ. On average, $\delta_{k,\lambda}$ was minimum for a linear surface ($k = 1$) and 25% of the pixels were regarded as stationary ($\lambda = 0.25$). In the ANOVA, both k and λ were found to be a significant factor in the response (both at levels $P < 0.001$), but the interaction between both proved insignificant ($P > 0.6$). Post hoc testing showed that the response was significantly lower for $k = 1$ and $\lambda > 0.10$. Hence, a linear surface ($k = 1$) with a noncritical stationarity percentile
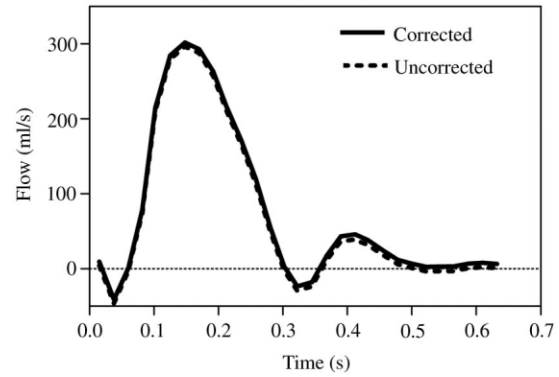
of 25% ($\lambda = 0.25$), gives optimal performance of the phase offset error correction method. A resulting selection of stationary pixels of two patients is shown in Fig. 2. As can be observed from the lower panel, most pixels in a ghosting band are automatically excluded.

Effect on Flow Quantification

Phase offset error correction significantly reduced the average error and removed the average bias in both mean velocity and mean volume flow. A pulmonary artery volume flow curve, before and after correction is shown in Fig. 5. Uncorrected, the average phase offset error in the mean velocity in the pulmonary artery as compared with the phantom acquisition at the same location was 0.76 ± 0.74 cm/second (mean $\pm$ SD). This is equivalent to a root mean square error ($= \sqrt{\text{mean}^2 + \text{SD}^2}$) of 1.1 cm/second. After correction, the error significantly reduced to -0.04 ± 0.35 cm/
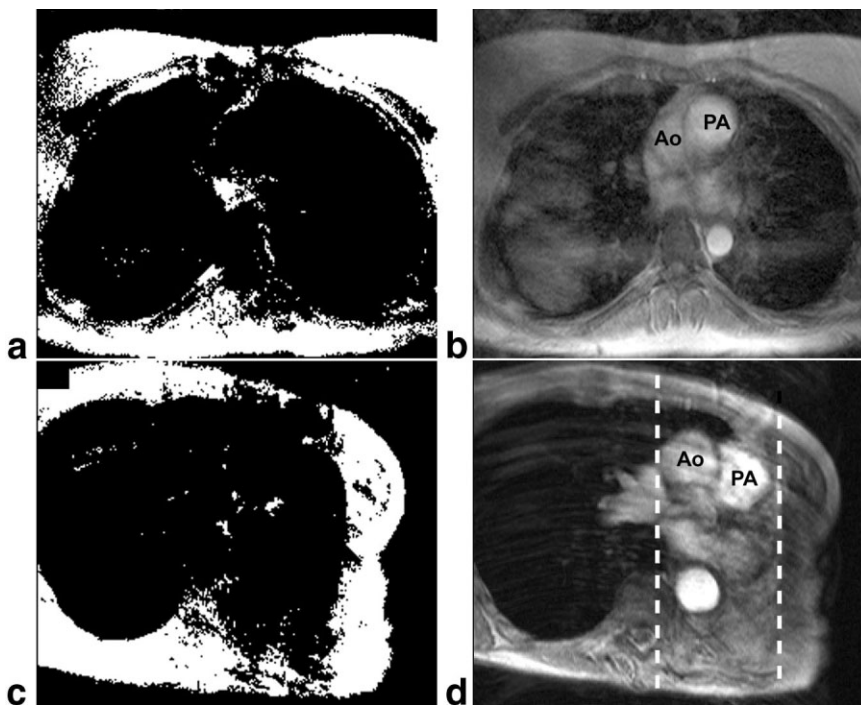

Figure 2. Selections of stationary pixels (white) in two patients (**a,c**; $\lambda = 0.25$). The corresponding magnitude images are also shown (**b,d**). Strong ghosting artifacts (d: visible in the area between dashed lines) are excluded from the selection automatically (c). Ao = aorta, PA = pulmonary artery.
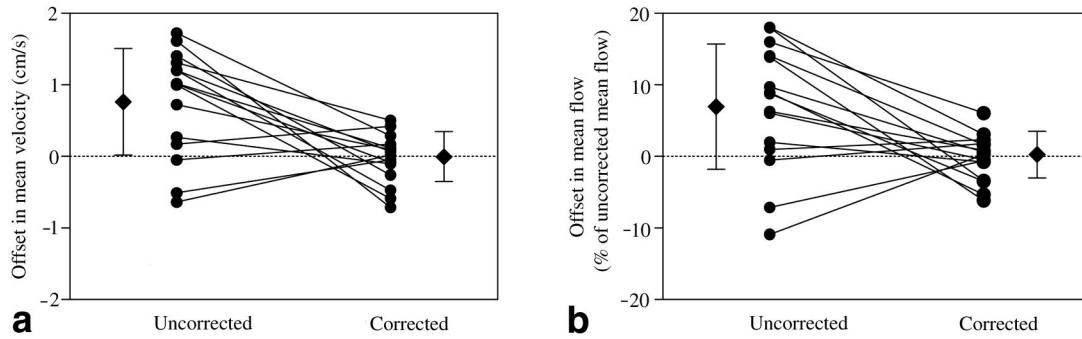
Figure 4. a: The phase offset error in the mean velocity in the pulmonary artery of all subjects before and after correction. **b:** The phase offset error before and after correction, presented as a percentage of uncorrected mean volume flow. Group mean and SD are shown.

second ($P < 0.01$), which is equivalent to a root mean square error of 0.35 cm/second. The uncorrected and corrected phase offset errors in the mean velocities of the individual subjects are shown in Fig. 6a. In two cases, the error in the mean velocity increased in absolute value after correction (from 0.17 to 0.42, and from −0.05 to 0.17 cm/second).

The mean volume flow before and after correction was 113 ± 35, and 104 ± 34 mL/second. To what extent phase offset errors and their correction affect mean volume flow in the pulmonary artery can be seen from Fig. 6b, in which the error in mean volume flow before and after correction is shown as a percentage of the uncorrected mean volume flow. Uncorrected, the error was on average $6.9 \pm 8.8\%$ of mean volume flow (range −11 to 18%), and after correction it was reduced to $-0.2 \pm 3.3\%$ (range −6.2 to 6.1%). This is equivalent to a reduction in root mean square error from 11 to 3.1% of mean volume flow. Stroke volume changed from an average of 85 ± 31 to 78 ± 31 mL. This corresponds to an average change of $7 \pm 11\%$ (range −11 to 26%). Thus, phase error correction strongly influenced stroke volume.

Check of Assumptions

The agreement between the phase offset error of pixels in stationary tissue and the corresponding phase offset
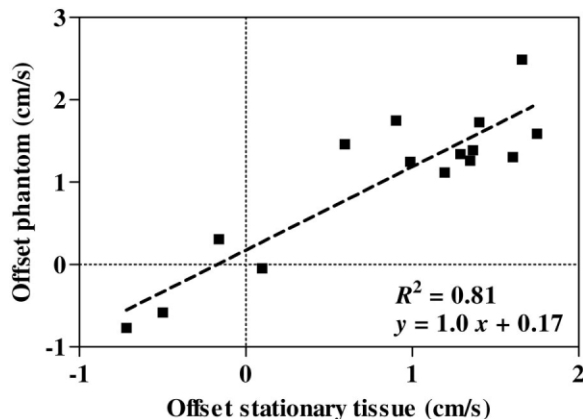

Figure 5. Average phase offset error of corresponding regions in stationary tissue and in the phantom acquisition.

error in the phantom is shown in Fig. 3. The phase offset error in stationary tissue correlated well with the phase offset error in the phantom ($R^2 = 0.81$; $P < 0.001$). Slope and intercept of the regression line did not differ significantly from 1 and 0, respectively. The SD of the residuals was equal to 0.41 cm/second.

Figure 4 shows the spatial average of the offset in all stationary pixels ($\lambda = 0.25$) as a function of the frame number in four subjects. In general, about the first 10 frames showed oscillations in all patients, whereas the rest of the cardiac cycle was stationary. Because the overall average was about equal to the diastolic value, the oscillations did not affect integrated parameters such as stroke volume and mean volume flow.

DISCUSSION

In this study, the performance of a time-independent variant of the method of Walker et al (6) for correction of phase offset errors in phase-contrast velocity quantification of pulmonary artery flow, was validated on an MR scanner equipped with a high-power gradient system. Application of the method in 15 subjects showed that correction with a first-order surface and 25% of the pixels regarded stationary, gave a significant reduction of the phase offset errors in pulmonary artery flow. In the investigated range (5–50%), the choice of the percentile of pixels regarded stationary did not turn out to influence the performance of the correction method as long as it exceeded 10%. The choice of the surface order, however, did. Our findings confirm the use of a linear surface, as was applied by Walker et al (6). Thus, application of this method is still valid when concomitant gradient terms have been compensated.

Compared with a phantom acquisition, application of the correction method reduced the average absolute velocity error from 1.1 to 0.35 cm/second. Thus, the accuracy is about equal to that of the separate phantom measurement. As a percentage of mean volume flow, the error was reduced from 11 to 3.1% on average. In none of the subjects, the error exceeded an absolute error of 6.3% of mean volume flow after correction. We regard this acceptable for clinical application.

The phase offset errors measured in a stationary phantom served as a reference for the phase offset error. In agreement with other studies (3,9,10), the phan-
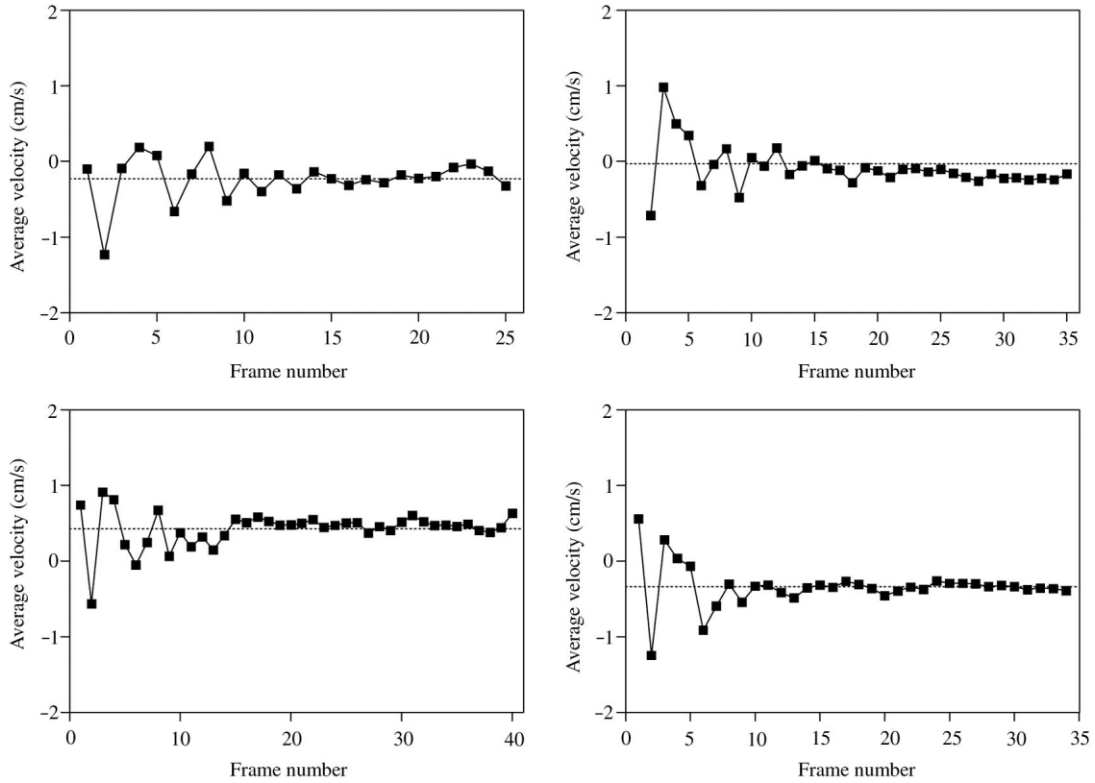
Figure 6. Average velocity per frame of the selection of stationary pixels (25% of the pixels regarded stationary) in four subjects. The dotted line denotes the overall average.

tom matched stationary tissue well although differences were found (Fig. 3). These differences may be attributed to disparities in eddy-current induction in the homogenous phantom fluid and in the heterogeneous human thorax. Also eddy-current fluctuations over time may play a role, but their influence was minimized by conducting the phantom acquisition directly after the subject acquisition. Though in individual cases differences may occur, on average no bias was found.

This study had several limitations. First, this study focused on correction of phase offset errors of a single MR scanner for a specific imaging plane with a single acquisition sequence. Strictly speaking, no conclusions can be drawn about other scanners, imaging planes and sequences. However, because the results confirm the validity of the method of Walker et al (6) in a different setting, it is likely that the method is also applicable in other settings. As stated before (6), the optimal percentile might be different for other applications with another slice position.

Second, in contrast to the original method of Walker et al (6), a time-independent surface fit was applied. We made this choice because we mainly focused on clinical use for noninvasive stroke volume quantification. In that case, the time-averaged volume flow is of more importance. We argued that fitting to time-averaged pixels would yield a better surface fit because of improved signal-to-noise ratio, which is especially important for fitting higher-order surfaces. For higher order surface fits, the number of parameters increases rap-

idly (e.g. a surface order of $k = 5$ is described by 21 parameters, see Eq. [3]). It turned out that a surface order of $k = 1$ (with three parameters) is optimal and that the assumption of stationarity of the phase offset error was somewhat violated in systole. However, as can be seen from Fig. 4, the overall average equals the diastolic value, thus these nonstationarities (due to eddy-current stabilization after the short scan delay due to prospective ECG triggering) do not significantly influence the time average. In retrospect, we conclude that a time-dependent fit might have been better, but because the phantom acquisitions were untriggered, we cannot really answer that question. Note that application of retrospective gating would also results in a more stable and time-invariant phase offset (14).

A more general limitation of this kind of correction methods is their sensitivity to spatial aliasing (infolding) artifacts. Because they should be manually removed from the selection of stationary pixels, the method cannot be implemented fully automatically. Full-automatic implementation is furthermore restricted by a possible dependence of the stationarity percentile on the application. Because human interaction thus cannot be excluded, it would be most suitable to implement the correction method in flow analysis software.

The clinical value of MR phase-contrast flow quantification depends heavily on the reliability with which parameters such as mean volume flow and stroke volume can be determined. The results of this study indicate that phase offset errors strongly influence these parameters. The average change in stroke volume was

$7 \pm 11\%$, with a maximum of 26%. Thus, phase offset errors have a large impact on stroke volume. For clinical use, this is undesirable, because it impairs flow quantification and its sensitivity for detecting changes (e.g. due to therapy or progression of a disease). This is especially important in patients with pulmonary hypertension. In these patients stroke volume may be low ($<$50 mL), but it may also be the only parameter that correlates with clinical improvement (15,16). The results of this study indicate that even in these patients, phase offset errors can be effectively reduced. It does so, without introducing an elaborate procedure (e.g., an extra phantom acquisition) or too much observer-dependency.

In conclusion, in this study, an existing method for correction of phase offset errors was evaluated in vivo using the pulmonary artery flow of 15 subjects. Using a linear surface fit, and regarding 25% of the pixels stationary, the average error in the mean volume flow was reduced to below 6.3%. Thus, phase offset errors remaining after compensation for concomitant gradients, can be effectively reduced on an MR scanner with a high-power gradient system.

REFERENCES

1. Bernstein MA, Zhou XJ, Polzin JA, et al. Concomitant gradient terms in phase contrast MR: analysis and correction. Magn Reson Med 1998;39:300–308.
2. Lotz J, Meier C, Leppert A, Galanski M. Cardiovascular flow measurement with phase-contrast MR imaging: Basic facts and implementation. Radiographics 2002;22:651–671.
3. Caprihan A, Altobelli SA, Benitez-Read E. Flow-velocity imaging from linear regression of phase images with techniques for reducing eddy-current effects. J Magn Reson 1990;90:71–89.
4. Pelc NJ, Herfkens RJ, Shimakawa A, Enzmann DR. Phase contrast cine magnetic resonance imaging. Magn Reson Q 1991;7:229–254.
5. In Den Kleef JJE, Groen JP, De Graaf RG. U.S.Philips Corporation. Method and apparatus for carrying out a phase correction in MR angiography. US Patent 4,870,361;1989.
6. Walker PG, Cranney GB, Scheidegger MB, Waseleski G, Pohost GM, Yoganathan AP. Semiautomated method for noise reduction and background phase error correction in MR phase velocity data. J Magn Reson Imaging 1993;3:521–530.
7. Greil G, Geva T, Maier SE, Powell AJ. Effect of acquisition parameters on the accuracy of velocity encoded cine magnetic resonance imaging blood flow measurements. J Magn Reson Imaging 2002; 15:47–54.
8. Danton MH, Greil GF, Byrne JG, Hsin M, Cohn L, Maier SE. Right ventricular volume measurement by conductance catheter. Am J Physiol Heart Circ Physiol 2003;285:H1774–H1785.
9. Keegan J, Firmin D, Gatehouse P, Longmore D. The application of breath hold phase velocity mapping techniques to the measurement of coronary artery blood flow velocity: phantom data and initial in vivo results. Magn Reson Med 1994;31:526–536.
10. Hofman MBM, Van Rossum AC, Sprenger M, Westerhof N. Assessment of flow in the right human coronary artery by magnetic resonance phase contrast velocity measurement: effects of cardiac and respiratory motion. Magn Reson Med 1996;35:521–531.
11. Markl M, Bammer R, Alley MT, et al. Generalized reconstruction of phase contrast MRI: analysis and correction of the effect of gradient field distortions. Magn Reson Med 2003;50:791–801.
12. MATLAB Mathematics. Natick, MA. The MathWorks; 2004. 349p.
13. Marcus JT, Vonk-Noordegraaf A, De Vries PM, et al. MRI evaluation of right ventricular pressure overload in chronic obstructive pulmonary disease. J Magn Reson Imaging 1998;8:999–1005.
14. Hofman MBM, Lankhaar JW, Van Rossum AC. Offset correction in MR phase contrast velocity quantification within the thorax. In: Proceedings of the 13th Annual Meeting of ISMRM, Miami Beach, 2005. (Abstract 1733).
15. D'Alonzo GE, Barst RJ, Ayres SM, et al. Survival in patients with primary pulmonary hypertension. Results from a national prospective registry. Ann Intern Med 1991;115:343–349.
16. Roeleveld RJ, Vonk-Noordegraaf A, Marcus JT, et al. Effects of epoprostenol on right ventricular hypertrophy and dilatation in pulmonary hypertension. Chest 2004;125:572–579.